Aus dem Institut für Medizinische Immunologie
der Medizinischen Fakultät Charité – Universitätsmedizin Berlin

DISSERTATION

Specificity Profiles of Protein Recognition Domains in the Molecular Medicine

zur Erlangung des akademischen Grades
Doctor rerum medicinalium (Dr. rer. medic.)

vorgelegt der Medizinischen Fakultät
Charité – Universitätsmedizin Berlin

von

Víctor E. Tapia Mancilla

aus Valparaíso, Chile

Datum der Promotion: .. 22.06.2014.....

Inhaltsverzeichnis

Zusammenfassung

ABSTRAKT

Diese Dissertation beschreibt zwei Forschungsprojekte, welche sich mit den Spezifitätsprofilen der molekularen Erkennung von nativen linearen Motiven durch Module der Proteinarchitektur befassen. Insbesondere handelt es sich um drei Tryptophan-Tryptophan Protein-Interaktions-Domänen (kurz: WW), die im Wildtyp der BAG3 und PQBP1 Proteine, als auch des Y65C mutierten PQBP1 vorkommen. Das mutierte Y65C PQBP1 Protein ist mit dem Auftreten des Golabi-Ito-Hall Syndroms assoziiert, einer X-verbundenen intellektuellen Behinderung (X-LID).

Der Sequenzraum, in welchem die Erkennungsspezifität der WW definiert wurde, entspricht einem Satz von 1885 Peptidproben aus dem human-proteomischen Repertoire potentieller Liganden. Zusätzlich, wurde eine unabhängige Kontrolle der kreuzreaktiven Bindungsereignisse durchgeführt. Dadurch war es möglich, jene Sequenzelemente zu identifizieren, welche eine Neigung zur Wechselwirkung mit dem Detektionssystem aufweisen und somit falsch positive Ergebnisse erzeugen.

CASA Projekt: Da BAG3 das einzige Mitglied der BAG ko-Chaperonen Familie mit einer WW in seiner modularen Architektur ist, wurde im ersten Projekt erwartet, dass ein Spezifitätsprofil der WW neue Einblicke liefere, um folgende Frage zu beanworten: Wie kann BAG3 das Schicksal von Hsc70-Substraten vom Abbau oder von der Renaturierung hin zur Chaperon-assistierten selektiven Autophagie (CASA) lenken? CASA ist von entscheidender Bedeutung für die Homöostase von Proteinfaktoren, die mechanischer Beanspruchung ausgesetzt sind.

Die Spezifität der BAG3-WW für lineare Motive wurde durch Peptidarrays kartiert. Dadurch wurden potenzielle Proteinelementen des CASA-Komplexes identifiziert und die Anhäufung an biologischen Prozessen im Spezifitätsprofil analysiert. Schließlich wurde die Rolle von CASA in filaminabhängigen mechanosensitiven Signalwegen und im Targeting von Hsc70-Sustraten für die Autophagie in glatten Muskelzellen, humanen Jurkat T Lymphoblasten und primären Leukozyten untersucht.

GIHS Projekt: Frühere Berichte belegen durch klinisch-genetische Analyse, dass das Golabi-Ito-Hall-Syndrom (GIHS) mit einer Y65C Punktmutation der WW von PQBP1 einhergeht. Die PQBP1-WW ist die einzige strukturierte Domäne, die in der modularen Architektur des Proteins

vorliegt. Mit dieser Beobachtung wurde im zweiten Projekt die Hypothese aufgestellt, dass durch die Y65C-Mutation die Erkennung von Schlüsselfaktoren eingeschränkt wird. Die Identifizierung dieser Faktoren könnte zur Offenlegung von wichtigen biologischen Prozessen in der molekularen Medizin der X-LIDs führen.

Um dies zu prüfen, wurden die Spezifitätsprofile beider WWs (Wildform und Y65C-Mutante) vergleichend analysiert, um somit probenspezifische Mutationseffekte zu identifizieren und als „loss-“ oder „gain-of-function“ zu klassifizieren. Eine Fokussierung auf die validierte PQBP1-Interaktion mit dem Spleißfaktor WBP11 (auch als SIPP1 bekannt), der einen starken loss-of-function Effekt zeigt, führte zur Vermutung, dass das GIHS durch die Deregulierung des pre-mRNA-Spleißens verursacht wird. Diese Hypothese wurde auf Lymphoblastenzellen von GIHS Patienten getestet.

ABSTRACT

This report describes two different research projects concerning the specificity profiles of native linear motif recognition by three modules of protein architecture, namely three WW protein interaction domains (PIDs) found in the wild-type forms of the proteins BAG3 and PQBP1, as well as in the X-linked intellectual disability (X-LID) associated Y65C point-mutation in PQBP1.

The sequence diversity space on which recognition specificity was defined for WW domains corresponds to a core set of 1885 peptide probes representing the human proteomic repertoire of potential ligands. Additionally, an independent control of cross-reactive binding events was carried out and used to describe sequence elements with potential to give false-positive measurements by interaction with three different detection systems in the absence of a specific analyte.

Firstly, since BAG3 is the only BAG-family member with a WW domain in its modular architecture, a specificity profile of proteomic PPXY recognition was expected to give new insights to explanations of how BAG3 diverts the fate of Hsc70-clients from co-chaperone assisted proteosomal degradation or renaturation to the co-chaperone assisted selective autophagy (CASA). CASA is known to be crucial for the homeostasis of protein factors, which sens mechanical stress.

The linear motif specificity of the BAG3-WW was mapped to identify potential protein recruits for CASA and to analyze the enrichment of biological processes in the specificity profile. Finally, the role of CASA in the transduction of filamin-dependent mechano-sensing and targeting of Hsc70

clients to autophagy was identified in tension-induced adherent A7r5 smooth muscle cells, human Jurkat T lymphoblasts, and primary leukocytes.

Secondly, early reports showed that the Golabi-Ito-Hall syndrome (GIHS) associated by clinical genetics to a Y65C point-mutation in the WW domain of PQBP1, the single structured domain in the modular architecture of the protein. This brought up the hypothesis that the identification of key factors with compromised recognition by the mutated WW domain could reveal important biological processes involved in the molecular medicine of X-LIDs.

For this, a comparative analysis of mutant versus wild-type WW specificity profiles of PQBP1 were applied to identify probe specific mutation effects and the enrichment of biological processes in probe classes with a different stamp of the mutation effect (loss- or gain-of-function). Focus on the known PQBP1 interaction with the splicing factor WBP11, which showed a strong loss-of-function effect, suggested that the Y65C PQBP1-associated X-LID syndrome is caused by deregulation of pre-RNA splicing. This hypothesis was tested on lymphoblast cells from GIHS patients.

INTRODUCTION

Specificity Profiles

Cellular function is usually explained in biology and medicine through models, in which a redundant or degenerate input is transformed into a meaningful pattern. A key concept of such explanations is the specificity of molecular recognition. In fact, the most often driving force behind the technological developments observed in high-throughput strategies to analyse molecular interactions, is to describe recognition specificity in terms of probability or affinity.

Despite the ubiquitous use of the concept, any attempt to define it has been as controversial as a definition of living systems (Pawson and Nash, 2000). Nevertheless, scientific debate about specificity, e.g. in cellular signal transduction, has lead to some delightful ideas around the apparent paradox between promiscuous binding events and functional outputs.

Instead of giving an absolute definition, which to my best knowledge is not satisfactorily given in the literature, focus is given here to a paradigm shift pointed out early by (Mayer, 2001) and others. The most widely used model to explain the functional outputs of cellular signal transduction is a correction of the most simplistic linear chain of binding events (Fig. 1A) through differential expression, sub-cellular compartmentalization, additive effects of multiple binding sites between inter-

action partners, and cooperative allosteric effects upon assembly of molecular complexes (Ladbury and Arold, 2000). While the linear-chain model relies on an affinity-driven concept of inherent specificity, corrections of it give account for the general observation that affinity for natural ligands may be comparable to that for competing ligands. The corrected linear-chain model relies in the concept of an effective specificity driven by the factors mentioned above.

Beyond corrections, a different model is mostly used in the analysis of molecular interaction networks. Therein, inherent specificity of pair-wise interactions is replaced by a network of interactions with dynamic equilibria for assembly to functional molecular complexes (Fig. 1B). The gain in information content that can be assigned to individual interactions in such a probabilistic view and its potential to explain the evolutionary plasticity of protein interactions (Beltrao and Serrano, 2007) is, in fact, very seductive.

The work described here takes a pragmatic position in this debate. The basic strategy consists in defining an in vitro context of extensive peptide probes to define specificity as a profile of biochemical binding potential based on semi-quantitaive data (inherent specificity) and validating selected potential interactors via pull-down and co-localization experiments (effective specificity). The modular analysis of specificity, i.e. focusing on interactions mediated by PIDs, was essential to investigate the individual problems of the two independent projects introduced subsequently.

BAG-Family Co-Chaperone Commitment in Proteostasis

Text from Ulbricht et al. (2013), see there for references.

Mechanical tension is an ever-present physical stimulus in cells and tissues. Cardiovascular, respiratory, urogenital, and locomotory systems are permanently exposed to mechanical stress and respond to mechanical signals under physiological and pathophysiological conditions. Even in settings without an explicit mechanical stimulus, crosstalk between the actin cytoskeleton, cell surface adhesion proteins such as integrins, and the extracellular matrix (ECM) generates mechanical tension, critical for processes ranging from inflammation to stem cell differentiation and oncogenic transformation. Sensing mechanical forces involves tension-induced conformational changes and unfolding of mechanosensors such as the ECM component fibronectin, integrins and different actin-anchoring proteins. A common response is the reinforcement of adhesion sites and of the actin cytoskeleton, which depends in part on the transcriptional regulators YAP and TAZ. Yet, how mechanosensing is ultimately linked to transcriptional responses remains poorly understood (Fig. 1C).

Chaperone-assisted selective autophagy (CASA) is essential for maintaining muscle activity under mechanical strain in flies, mice and men. Impairment of CASA causes severe childhood muscular dystrophy and dilated cardiomyopathy, and was linked to limb-girdle muscular dystrophy. CASA operates at the Z-disk, a protein assembly for actin-anchoring in striated muscles. It initiates the lysosomal degradation of Z-disk components such as the integrin-binding and actin-crosslinking protein filamin, following contraction induced unfolding and damage. Unfolded filamin is recognized by a chaperone complex containing heat shock cognate Hsc70 and the small heat shock protein HspB8 (also known as Hsp22), which are physically linked by the CASA-inducing co-chaperone BAG3. Filamin is released from the Z-disk, becomes ubiquitylated by the Hsc70-associated ubiquitin ligase CHIP and is directed towards the lysosomal compartment in a manner dependent on the autophagic ubiquitin adaptor p62. Autophagic degradation of filamin is a prerequisite for maintaining Z-disk architecture under mechanical strain.

Ulbricht et al. (2013) shows the role of BAG3 in linking mechanosensing to YAP/TAZ signalling and recruitment of the CASA-client filamin to lysosomes. It also shows that CASA is not restricted to striated muscles but instead is part of a common mechanotransduction pathway, which senses mechanical unfolding, maintains responsiveness to mechanical cues by exploiting protein homeostasis mechanisms, and triggers transcriptional responses to cope with mechanical strain.

The Intriguing Role of PQBP1 in X-LID

Text from Tapia et al. (2010), see there for references.

The PQBP1 (polyglutamine tract-binding protein 1) gene encodes a nuclear protein of 38 kDa that is abundantly expressed in the central nervous system. Several studies have provided evidence for a role of the PQBP1 protein in the pathogenesis of polyglutamine expansion diseases, including spinocerebellar ataxia type 1. More direct evidence for the contribution of PQBP1 to neurological disorders has come from clinical genetics. Mutations in the PQBP1 gene were reported in several X chromosome-linked intellectual disability (X-LID) disorders, such as Renpenning, Sutherland-Haan, Hamel, Porteous, and Golabi-Ito-Hall syndromes (GIHS). Interestingly, although caused by different mutations within the PQBP1 gene (e.g. frame shifts that result in truncated protein products, missense point mutation; see Fig. 1D and E), these syndromes share similar clinical features. In addition to severe intellectual disability, the patients also have a short stature, lean body, small head, and are frequently diagnosed with cardiac abnormalities (atrial septal defects).

The missense mutation in the GIH syndrome (Fig. 1D) is unique among the PQBP1 mutations reported so far because it maps within the single structured region of the protein known as the WW domain and because the lesion does not affect the size of the mutated protein. The WW domain is a well characterized PID that mediates specific interactions with ligands that contain short proline-rich motifs. The domain is composed of 38 amino acids, and it is one of the smallest among all PIDs. The structure is a three β-strand meander that forms a shallow binding pocket for proline-rich ligands. In general, the folding of WW domains does not require cognate ligands or co-factors.

The WW domain of PQBP1 was shown to interact with the pre-mRNA splicing factor WBP11, also known as SIPP1, and with RNA polymerase II. Consequently, the PQBP1 protein was suggested to regulate pre-mRNA splicing and transcription. The WW domain mutation implicated in GIHS results in a chemically significant substitution by changing the conserved tyrosine at position 65 within the aromatic core of the domain to cysteine. Mutations that locate within PIDs or in their cognate ligands have been shown to affect the complexes and result in diseases.

Therefore, we hypothesized that the Y65C mutation of the PQBP1-WW domain would lead to a loss or gain of function by affecting the binding of the domain, and ultimately of the protein, to cognate ligands. We also considered that the mutation could affect the folding and stability of the protein. We tested our hypotheses by a number of complementary biochemical, biophysical, and cell biology techniques. Our data show that the binding function of the mutated domain is affected, as assayed by in vitro screens of peptide repertoires that represent the complete proteomic complement of PPXY motif-containing human proteins.

Selected proline-rich peptides derived from known protein partners of PQBP1 WW domain, including that of WBP11, were used in binding assays and showed that the Y65C mutation resulted in decreased binding of the domain to these peptides. Moreover, we documented that the compromised complex between PQBP1 and WBP11 resulted in the pre-mRNA splicing defect in GIHS-derived lymphoblasts but not in the control cells. We also found suggestive evidence that the Y65C mutation affected folding of the mutated protein, but apparently it did not change the rate of protein degradation. Our report sheds light on the molecular consequence of the missense mutation that causes GIHS and provides guides for further molecular analysis of PQBP1 function.

METHODS

A selection of analytical approaches essential for comprehensiveness of this report is described below. For reproducibility please refer also to the preparative approaches in the original publications.

CONTROL OF UNSPECIFIC ANALYTE CAPTURE

Berlin – Blank analyte constructs were prepared by standard SPPS. Constructs consisted in the GGG tripeptide cojugated to either FITC, biotin, or TAMRA. Biotin-tagged constructs were complexed with SA-HRP fusion proteins for detection. Peptides probes to test unspecific binding to the above stated detection systems were designed as GGGGXXXXGGGG, where X is any of 20 natural aminoacids or a library of stochastic sequences. For details, please refer to (Mahrenholz et al., 2010).

SPECIFICITY PROFILES

Berlin – Spot membranes in Figure 4 were incubated for 24 h in 10 mm Tris-HCl at pH 7.5, 150 mm NaCl, 0.1% Triton X-100, 0.1 mm reduced glutathione, 1× Sigma blocking buffer with of 32P-labelled GST-WW domain of PQBP1 (WT or Y65C mutant). For labelling of the probes, 10 µg of each fusion protein were used following the published protocol (Tapia et al., 2010). Dried membranes were exposed to Kodak x-ray films without using screens.

The preparation and handling of the membrane in Figure 2A was performed as described in (Ulbricht et al., 2013). HRP-SA/biotin-WW complexes captured by peptide probes were revealed by enzyme-linked turnover of luminol in a HRP substrate-mix (SuperSignal West Pico, Thermo Scientific Pierce Inc.), and recorded on a Lumi-ImagerTM F1 Workstation (Roche Applied Science) to a digital image.

Values of SI from datasets were ordered by the rank index k ranging from 1 (highest SI) to N (lowest SI), where N is the total number of screened probes. Thresholds were defined by specifying a value of k and reading the corresponding signal intensity of the k-ranked probe, i.e. a k=100 threshold means that 100 peptide probes are defined over the threshold. In Figure 2, this index corresponds to a SI100=12296 AU, which is equivalent to the median background intensity plus 24 times SD.

FOLDING ANALYSIS OF PQBP1-WW DOMAIN VARIANTS

Berlin & London – Circular dichroism (CD) measurements were performed on a Jasco J-715 spectropolarimeter equipped with a PTC-348 Peltier system for temperature control. The instrument was calibrated with d-(+)10-camphorsulphonic acid. Protein concentrations of 60 and 150 µm and quartz cuvettes with path lengths of 1 and 2 mm were used for recording far- and near-UV spectra, respectively. Thermal unfolding experiments were performed by recording the dichroic signal at 230 nm in the temperature range of 5–95 °C. The samples were heated at a rate of 1 °C/min and successively cooled down to 10 °C to determine reversibility.

Steady-state fluorescence measurements were performed on a SPEX Fluoromax spectrometer by exciting protein samples at 295 nm (slit width, 0.4 nm) and recording the emission intensity from 300 to 450 nm (slit width, 1.5 nm). All data were evaluated using the ORIGIN program package (Micro-Cal Software).

EX VIVO BINDING ASSAYS OF PQBP1 & WBP11

New York – Human embryo kidney 293 (HEK293) cells were transfected with expression vectors that encode the protein of interest using Lipofectamine (Invitrogen). 24 h later, cells were lysed with modified immune precipitation assay buffer (50 mM Tris-HCl, pH 7.45, 5 mM EDTA, 300 mM NaCl, 1% glycerol, 1% Triton X-100, 0.1% sodium deoxycholate, 0.1% SDS) and immunoprecipitated using anti-FLAG M2 affinity gel (Sigma). The immunoprecipitates were washed with the modified immunoprecipitation assay buffer. Bound proteins were separated by SDS-PAGE followed by immunoblotting.

For further immunoprecipitation experiments, exponentially growing lymphoblast cells and transfected HEK293T cells were washed twice with phosphate-buffered saline and harvested in a lysis buffer containing 50 mM Tris-HCl at pH 7.5, 0.3 M NaCl, 0.5% (v/v) Triton X-100, 0.5 mM phenylmethylsulfonyl fluoride, 0.5 mM benzamidine, and 5 μM leupeptin. The homogenates were centrifuged for 10 min at 10,000 ϫ g, and the supernatants (cell lysates) were used for immunoprecipitation. Anti-EGFP (enhanced GFP) or anti-HA antibodies were added for 1 h at 10 °C followed by incubation with Protein-A-TSK-SepharoseTM for another hour. Before immunoblotting, the precipitates were washed once with TBS (20 mM Tris-HCl at pH 7.4 plus 150 mM NaCl) containing 0.1 M LiCl, twice with TBS supplemented with 0.1% Nonidet P-40, and once with 20 mM Tris-HCl at pH 7.4.

EX VIVO BINDING ASSAYS OF BAG3 & SYNP2

Bonn – To localize the BAG3 binding site on filamin, His-tagged filamin C (FLNC) fragments were immobilized on Ni-NTA agarose (Qiagen) at ~0.5 μg protein per μL resin. 10 μL of the affinity resin were incubated with BAG3 at a concentration of 1 μM in 250 μL washing buffer (20 mM MOPS-KOH, pH 7.2, 100 mM KCl, 60 mM imidazole) for 1 h at 4°C, followed by six washing steps with the same buffer. Retained proteins were finally eluted with elution buffer (20 mM MOPS-KOH, pH 7.2, 100 mM KCl, 200 mM imidazole). Eluted proteins were precipitated in 10% trichloroacetic acid and analyzed by immunoblotting. When binding of CASA components to Ig19-21 of filamin was analyzed, His-Ig19-21 (1 μM) was incubated with BAG3, GST, GST-HspB8 or

Hsc70 (1 μM of each) as indicated for 1 hour at 4°C in the presence of Ni-NTA agarose, followed by the experimental steps described above.

For analysis of the SYNPO2-BAG3 interaction, His-tagged SYNPO2 fragments were immobilized on Ni-NTA agarose and incubated with BAG3 and BAG3 WAWA. Binding experiments were performed as described above. To analyze binding of the SYNPO2 PPPY domain to BAG3, MBP- PPPY or MBP were incubated with BAG3 (1 μM of each) in washing buffer (20 mM MOPS-KOH, pH 7.2, 100 mM KCl, 0.5% Tween20) for 1 h at 4°C. Subsequently, BAG3 antibody was added (10 μg/ml) along with protein G-sepharose, and samples were incubated for 1 h at 4°C. Following six washing steps with washing buffer, bound proteins were eluted with glycine-HCl, pH 3.5 and analyzed by immunoblotting.

DUAL REPORTER ASSAYS

Leuven – Lymphoblast cells were transfected with the pTN24 reporter plasmid. After 48 h the cells were harvested in passive lysis buffer (Promega), and the lysates were used for the assay of luciferase and ß-galactosidase activities. The luciferase activities were measured with a Luminoskan Ascent luminometer (Labsystem) using the Promega Luciferase kit. The ß-galactosidase activities were measured using ortho-nitrophenyl-ß-galactosidase as substrate. The splicing efficiency was also determined by RNA analysis. Details as described in (Nasim and Eperon, 2006).

CELL STRETCH EXPERIMENTS

Jülich – For cell experiments on defined substrate elasticity, A7r5 cells were seeded on soft silicone rubber substrates as described before (Dupont et al., 2011; Fu et al., 2010). Elastomeric chambers were produced from a 40:1 mixture of base to cross-linker of Sylgard 184 (Dow Corning), which was filled in chamber molds and cured at 60°C for 16 h to receive a Young's modulus of 50 kPa. For softening the top layer of stretching chambers recognized by cells after adhesion, an approximately 100 μm thick layer of a 70:1 mixture (Sylgard 184) of soft silicone rubber (1.5 kPa) was prepared on the 50 kPa stiff chamber bottom. Mechanical properties were measured by indentation with a flat cylindrical punch (4 mm diameter). This indenter was attached to a force sensor (KD78 0.5 N; ME-Meßsysteme) and moved by a linear translation stage (PICO Linear Axis LTP 60; Steinmeyer-FMD). Indentation was performed in four successive steps each followed by a relaxation period of 40 min. Punch retraction was done identically. Step height was 200 μm for very soft elastomers (0.6 to 5 kPa) and 40 μm for stiffer ones (above 5 kPa). Forces were sampled at 10 Hz. For each step indentation resistance was calculated as ratio of equilibrium force (mean over the last 4 minutes) and indentation depth (step height corrected for the stiffness of the force sensor). For con-

version of indentation resistance values into Young's moduli we exploited the firmly established fact that indentation resistance is directly proportional to Young's modulus if geometry and Poison's ratio of the material are kept constant. By this method, Nusil 2.2:1 mixture recieved a Young's modulus of 0.6 kPa and for the 1:3 mixture 230 kPa.

A7r5 smooth muscle cells were seeded 12 hours before experimental start in 1.5 kPa soft elastomeric chambers at a density of 2,500 cells/cm2. Cells were stretched with an amplitude of 20% and a frequency of 130 mHz for 3 h followed by lysis in RIPA buffer (25 mM Tris-HCl, pH 8.0, 150 mM NaCl, 0.5% sodium deoxycholate, 1% Nonidet P-40, 0.1% SDS, 10% glycerol, Complete protease inhibitor (Roche)).

RESULTS

Chaperone-Assisted Selective Autophagy (CASA).

The CASA-inducing co-chaperone BAG3 contains a WW domain at its amino terminus. Such domains are known to interact with proline-rich motifs in binding partners (Sudol et al., 2001). To identify BAG3 interactors, a peptide array displaying 2296 proline-rich peptides from the human proteome was incubated with the BAG3 WW domain (Fig. 2A). The approach led to the identification of the known BAG3 binding partner RAPGEF6 (Iwasaki et al., 2010) and 100 putative BAG3 WW interactors, and revealed preferential binding of the domain to PPPY and PPSY motifs (Fig. 2C to E). One of the putative interactors was synaptopodin-2 (SYNPO2; also known as myopodin), a Z-disk localized adaptor protein in muscles and tumor suppressor in bladder and prostate (Fig. 2B).

WW domains and PPXY motifs are interaction partners involved in many components of the Hippo signalling pathway that controls organ growth and tumorigenesis (Bao et al., 2011). Among them are the transcriptional co-activators YAP and TAZ (WW domains) and the YAP/TAZ inhibitors LATS1/2 and AMOTL1/2, which contain PPXY motifs (Sudol, 2010; Sudol and Harvey, 2010). Intriguingly, the YAP/TAZ inhibitors LATS1, AMOTL1 and AMOTL2 were detected as potential BAG3 WW domain interactors in the peptide array screen (Fig. 2B). BAG3 might use its WW domain for binding PPXY-containing YAP/TAZ inhibitors and thereby induce YAP/TAZ release and activation.

Beyond these findings, the specificity profile of the BAG3 WW led to the successful identification of 72 proteins containing the 100 most reactive probes. 32% of such proteins were classified as having varied roles in cellular signal transduction and endocytosis. 8% are factors of ubiquitin-de-

pendent degradation and 22% interact with such factors. Finally, 7% of the identified potential interactors of BAG3 were factors of autophagy (Fig. 2F).

Extensive validation experiments by cooperation partners in Bonn and Jülich are partially shown in Fig. 3. Credits to respective labs are given in METHODS (see also affiliations in Ulbricht et al., 2013). Firstly, attention was focused on SYNPO2. In muscle cells four different isoforms of SYNPO2, i.e. SYNPO2a to d, are expressed, which all contain the PPPY motif recognized by the BAG3 WW domain. SYNPO2 isoform d lacks a C-terminal PDZ domain (Fig. 3A). Binding studies confirmed a WW-PPPY mediated interaction between BAG3 and SYNPO2 (see Fig. 1 in Ulbricht et al., 2013). Moreover, BAG3 was readily detectable in endogenous SYNPO2 complexes immuno-precipitated from rat smooth muscle cells (Fig. 3B). The CASA components Hsc70 and p62, and the CASA substrate and known SYNPO2 interactor filamin were also found associated with SYNPO2 (Fig. 3B). SYNPO2 apparently interacts with the CASA machinery by utilizing its PPPY motif for binding to the BAG3 WW domain.

To investigate the functional requirement for SYNPO2 during CASA, the BAG3 and SYNPO2 proteins were depleted from smooth muscle cells. Consequences for autophagosome (AV) and autolysosome (AL) formation were analyzed using a "traffic light" reporter of the autophagosome marker LC3B. In autophagosomes a tandem arrangement of the fluorescent proteins mCherry and eGFP gives rise to yellow fluorescence of the reporter, which turns red upon transfer to the more acidic (auto-)lysosomes due to eGFP quenching. Depletion of SYNPO2 isoforms, although incomplete, led to a 60-70% decrease in autophagosome formation, similar to the decrease observed upon BAG3 depletion, whereas autophagosome-lysosome fusion remained unaffected (Fig. 3B and C). CASA is apparently the prevalent autophagy pathway in adherent smooth muscle cells under normal growth conditions, and autophagosome formation during CASA critically depends on PDZ-containing SYNPO2 isoforms.

Given the enrichment of cell signaling factors in the PPXY specificity profile, attention was given to the identified components of the Hippo signaling pathway. YAP and TAZ are essential for mechanotransduction in response to extracellular matrix stiffness (Dupont et al., 2011). Targets of the transcriptional co-activators include the connective tissue growth factor CTGF, integrin ß2 and filamin, the expression of which is induced upon YAP/TAZ activation. On the other hand, activation can be blocked by retaining YAP/TAZ in the cytoplasm, either through binding to AMOTL1/2 or by an interaction with 14-3-3 proteins following LATS1/2-mediated phosphorylation of YAP/TAZ (see cartoons in Ulbrich et al. 2013 and literature cited therein). Indeed, LATS1 and

AMOTL1 were found to co-precipitate with BAG3 (Fig. 3F), and to be essential for full YAP/TAZ activation in adherent cells (see Fig. 4 in Ulbricht et al. (2013)), in agreement with a role of the CASA-inducing co-chaperone in transcription regulation.

To better define the crosstalk between CASA and YAP/TAZ regulation a previously established assay for YAP/TAZ activation under mechanical tension was adopted (Dupont et al., 2011). In this assay the actin cytoskeleton is subjected to different levels of tension by plating smooth muscle cells on fibronectin-coated elastomer substrates with varying stiffness, i.e. 1 kPa versus 100 kPa. Remarkably, high tension triggered a 3-fold increase in autophagosome number and induced LC3 lipidation, leading to increased LC3-II levels (Fig. 3G to I). Autophagy induction was accompanied by an elevation of BAG3 expression (Fig. 3I). The data identifies CASA as a tension-induced autophagy pathway and reveals a dual function of BAG3. The co-chaperone regulates degradation and transcription and thus emerges as a key proteostasis factor in mechanically strained cells.

Golabi-Ito-Hall Syndrome (GIHS)

To assess the effect of the Y65C mutation within the WW domain of PQBP1 on the binding function of the domain, the repertoire of PPXY motif containing 12-mer peptides that represent the entire human proteome was screened. In addition, 59 proline-rich peptides that did not contain the PPXY motif but scored positively in the proteomic map of the WW domain completed by the AxCell company (Hu et al., 2004) were included. The total of 1,958 peptides were synthesized on cellulose membranes using the Spot technique and probed with radioactively labeled GST-PQBP1-WW wt or GST-PQBP1WW Y65C mutant. No dramatic differences in the recorded pattern of spots associated to binding of the wt versus the Y65C WW domain were detected, although it can be observed that the majority of peptide probes bound more strongly to the wt domain than to the mutant WW domain (Fig. 4A). Using densitometric scanning, the relative intensity of the signal for each peptide spot was measured and the observed trend was confirmed by a correlation of the Y65C to the wt dataset of $r^2=0.80$ (similar profile) and an inclination of the correlation line of $m=0.70$ (weaker intesities measured for the Y65C dataset, Fig. 4B).

Measurements were ranked and the k most reactive spots across both datasets were selected. This approach identified a number R(k) of reactive probes, defined as having at least one reactive spot across both datasets. Then, to determine the mutation effect upon binding, reactive probes were grouped into a lost-of-function (LOF), a conserved (cons.), and a gain-of-function (GOF) group depending on which dataset they were reactive. LOF, cons., and GOF scores were counted and normalized to the number of probes represented in the complete library. Fig. 4C shows that

such scores were dependent on R(k). Nevertheless, for all values of R(k) GOF score ratios were no greater than 10% and LOF score ratios varied from 70 to 30%. Variations in GOF were compensated mostly by the cons. score ratio. This shows that, for any value of R(k), gain-of-function is the preponderant Y65C mutation effect upon WW-mediated linear motif recognition. For R(k=500), LOF and GOF scored at ratios of about 45 and 5%, respectively.

WW domains have been grouped in classes based on partial sequence similarity and binding specificity (e.g. (Hu et al., 2004) and (Otte et al., 2003)). Later factor, concerns mostly the X position in the PPXY motif. Owing the relevance of this position, the distribution of LOF and GOF scores in each PPXY-class was analyzed, identifying PPPY, PPRY, and PPHY as the most often and most strongly recognized peptide core motifs (Fig. 4D, grey line). At R(k=500), GOF scored at ratios of 100, 40, and 40% of recognized probes, respectively (Fig. 4D, straight line), while LOF scored always less than 5% (Fig. 4D, dotted line). It is thus evident that GOF preponderance is maintained across PPX-classes, although this may vary greatly especially for less strongly recognized peptide core motifs. Intriguingly, comparing the sequence specificity of the 25 most pronounced LOF probes (Fig. 4E) and the 25 most pronounced GOF probes (Fig. 4F) shows that proline fails to be represented in positions flanking the core motif, indicating a promiscuitive ligand recognition associated with the Y65C-mutant WW domain.

The above statements about PPXY-class specificity and the fact that the WW domain of PQBP1 recognizes diverse proline-rich motifs without aromatic residues suggests a versatile specificity profile of linear motif recognition. Therefore, the WW domain of PQBP1 belongs to those domains that show mixed ligand predilections and may be classified as Class I, II, and III WW domains. Alternatively, the PQBP1 WW specificity profile defies orthodox readouts of the classification paradigm.

The above observation was reproduced on a smaller set of selected probes using synthetic constructs of both versions of PQBP1 conjugated directly to TAMRA (see supplements in Tapia et al., 2010) or indirectly to HRP (Volkmer et al., 2012). The different detection systems applied in such reproduction experiments were systematically controlled for cross-reactive recognition of strictly and randomly defined physico-chemical groups of probes (Mahrenholz et al., 2010). Furthermore, taking account of PQBP1 binding to RNA pol II in phosphorylation-dependent fashion (Okazawa et al., 2002), the cellulose-supported peptide synthesis was firstly optimized for effective coupling of phosphorylated amino acid derivatives (Tapia et al., 2008), and then applied to produce a probe array containing complete permutations of phosphorylated positions of a canonical version of the 52

heptapeptide repeats (YSPTSPS) in RBP1 that are essential for polymerase activity (see supplements in Tapia et al., 2010). Biophysical analysis of binding to selected probes, aggregation at the lab of Klaus Gast (University Potsdam), and thermal renaturation at the lab of Sandro Keller (FMP, Berlin-Buch) were carried out by the author, and also by co-operation partners in London (see Tapia et al., 2010, for affiliation details).

Again here, validation via sagacious molecular biological and cell assays were carried out by co-operation partners. For details on credits to respective labs, see the section for methods and affiliations in Tapia et al. (2010). Firstly, beyond the fact that PIDs are autonomous structural and functional elements of protein architecture, the protein context in which they are immersed may have an important allosteric role. To test if a LOF-effect of the Y65C PQBP1 mutation holds true in a comparison of full length proteins, PQBP1 variants were transiently co-expressed with WBP11 in HEK 293T cells (Fig. 5A). Clearly, co-immunoprecipitation of EGFP-WBP11 was observed upon co-expression with HA-PQBP1, but not with the respective Y65C PQBP1 mutant fusion construct. Likewise, an interaction between endogenous PQBP1 and WBP11 could not be detected by co-immunoprecipitation analysis in a lymphoblast cell line from a patient with GIHS, but could be readily visualized in lymphoblasts from a healthy person, matched for age, gender and race (Fig. 5B).

Following the rationale of PQBP1 binding to the splicing factor WBP11, a dual reporter assay (Nasim and Eperon, 2006) was applied to provide a functional read-out of pre-mRNA splicing in GIHS cells. A TN24 reporter plasmid contains sequences encoding β-galactosidase as well as luciferase that are separated by an intronic sequence with multiple stop codons (Fig. 5C). When the primary transcript is not spliced, it generates β-galactosidase, whereas a fusion of β-galactosidase and luciferase is generated only after splicing. Thus, the luciferase/β-galactosidase ratio reflects the splicing efficiency. The transcript levels of the TN24 reporter were controlled by reversed transcription-PCR (RT-PCR) in lymphoblast cells from control and GIHS patients, as well as from control persons with small interfering RNA-mediated knocked-down PQBP1 (Fig. 5D). While similar pre-mRNA levels are observed across samples, GIHS samples reveal lower mRNA levels even resembling siPQBP1 samples (Fig. 5D and E). The siRNA-mediated knock-down of PQBP1 in the control lymphoblasts was verified by immunoblotting (Fig. 5F), showing the extent of compromised PQBP1 expression. On the dual reporter assay (Fig. 5G), GIHS lymphoblasts showed a more than 80% decay in splicing efficiency, as compared with the control cells, and resembled the effect of control cells with knocked-down PQBP1.

DISCUSSION

The inherent specificity of three WW domains was described as the probability to bind a set of peptide probes, which is designed to represent the human proteomic repertoire of PPXY motifs. The reliability of exploring analyte binding potential through such extensive sets of probes, has been determined (Weiser et al., 2005). Taking account of the semi-quantitative nature of data harvested from these experiments, it is essential to make one-border decisions with a safe threshold, e.g. through the specificity profile approach described in the methods section.

Moreover, given the sequence diversity of probes, efforts were undertaken to control false-positive measurements caused by cross-reactivity of the detection systems. This was specially important for the GIHS joint venture, where three basically different detection systems were applied (RIA with 32P-labelled GST, TAMRA fluorescence, as well as HRP-linked luminol turn-over). This was useful to point-out potential false-positive measurements by failing to group in the overlap of the respective datasets.

Such assessments are not viable for extensive exploratory assays. For such cases, as the ones concerning the present report, an independent control was designed to reveal sequence elements with cross-reactive potential to different detection systems (Mahrenholz et al., 2010). Peptide probes were challenged to GGG-fused FITC, TAMRA, and biotin/streptavidin-HRP. Then, probe sequences in Fig. 4A with enrichment of the cross-reactive elements to biotin/streptavidin-HRP were excluded from the list of potential ligands.

The specificity profiles identified short linear motifs from validated natural interactor proteins as well as new motifs. Indeed, while the success of the CASA project relied in the identification of new factors and led to original findings (Ulbricht et al., 2013), the success of the GIHS project was based in the comparison of the wt and Y65C profiles of PQBP1 WW linear motif recognition with further follow-up of the effect with biophysical and molecular-biological validation experiments (Tapia et al., 2010) focusing on the well described PQBP1/WBP11 interaction.

Ulbricht et al. (2013) reports the first involvement of CASA in the homoeostasis of mechanically stressed structures beyond Z-disks of striated muscle cells. The novel BAG3 interactor SYNPO2 was shown to effectively bind the BAG3 WW domain and co-precipitate other factors of the CASA machinery (Fig. 3B). Moreover, its depletion resulted in a decrease of autophagosomes (Fig. 3D and E). The novel PDZ- mediated interaction of SYNPO2 with VPS18 further involves CASA in autophagosome formation and client transport to lysosomes.

YAP/TAZ activation of filamin expression under mechanical stress was already an established fact (Dupont et al., 2011; Wada et al., 2011). YAP/TAZ can be blocked by WW- recognized inter action with AMOTL1/2 and LATS1/2 proteins, thus the identification of the later factors as BAG3 interactors lead to a postulation of BAG3 as a positive regulator of filamin transcription. The postulate argues that BAG3 sequesters the blocking factors leading to activation of filamin expression via YAP/TAZ. Cell-stretch assays showed that tension induces a ca. 2.5-fold in autophagosome counts in a manner dependent on BAG3 and SYNPO2. The observation that filamin transcript levels were ca. 3-fold increased under tension, while filamin protein levels maintained, rounds up a plot. Therein, BAG3 features a dual role in CASA-mediated transcription regulation and degradation of client molecules to maintain cellular structures under mechanical stress.

On the collaborative project concerning the role of PQBP1 in X-linked intellectual disability (X-LID), the inherent specificity of the wild-type and the Y65C-mutant PQBP1 WW were directly compared (Tapia et al., 2010). The collection of probes used to profile the linear motif recognition specificity contained a core repertoire of PPXY motifs and an additional tailor-made collection of non-PPXY potential ligands based on the literature. An independent comparison of the specificity of both WW versions was also carried out. Therein, the repertoire of probes represented a complete and redundant permutation of poS postitions in a sequence consensus of the CTD repeats in the human RNAPII (YS_2PTS_5PS-YS_2PTS_5PS).

Earlier reported interactions with phosphorylated CTD from RNAPII (Okazawa et al., 2002) and with SIPP1, a splicing factor interacting with Ser/Thr phosphatase-1 (PP1) protein (Llorian et al., 2005), were confirmed. Moreover, a comparison of wt and Y65C-mutant PQBP1 WW specificity profiles shows that the mutation, known to be associated with GIHS (Lubs et al., 2006), compromises the recognition of SIPP1. This effect was accordingly observed in cell extracts from HEK98 and lymphoblasts isolated from a GIHS patient (Figure 5A and B). Biophysical analysis of the mutation effect additionally showed a compromised thermal stability of the WW structure and reduced binding to SIPP1.

The consequences of the compromised PQBP1/SIPP1 complex was a significant reduction of pre-mRNA splicing, as shown in lymphoblasts derived from a GIHS patient. The decreased splicing efficiency was similar to that seen after small interfering RNA-mediated knockdown of PQBP1, indicating that PQBP1-Y65C is inactive in intact cells (Figure 5C-G).

Moreover, Tapia et al. (2010) shows that the known WW-mediation of binding to RNAPII (Okazawa et al., 2002) depends on hyperphosphorylation of RNAPII's CTD. In the cell this is done by the pTEFb kinase complex, which thus imprints a post-translational marker for elongating RNAPII, known to recruit splicing factors (Batsché et al., 2006; Phatnani and Greenleaf, 2006). The orchestrating role of RNAPII in the cross-talk between transcription and splicing is well described (Bird et al., 2004; David and Manley, 2011; Neugebauer, 2002).

These findings provide additional empirical support for a role of PQBP1 in pre-mRNA splicing. Alternative splicing is particularly important in the brain, and a switch in alternative splicing patterns of primary transcripts encoding neuron-specific proteins is known to accompany neuronal differentiation (Fairbrother and Lipscombe, 2008; Lipscombe et al., 2013). Changes in alternative splice choices could, therefore, represent an important factor in the etiology of GIHS. More details in the involvement of PQBP1 and alternative splicing in neurodegeneration could be achieved upon identification of primary transcripts targeted by PQBP1-assisted alternative splicing (Wang et al., 2013).

The diverse lesions in PQBP1 may lead to similar intelectual and morphological symptomes. Besides the Y65C point-mutation, all other X-LID associated PQBP1 mutation produce truncated proteins, which lack a C-terminal intrinsically unstructured domain known to bind the spliceosome assembling factor U5-15kDa. Such facts suggest that the WW domain of PQBP1 is sufficient to cause X-LID but not exclusively necessary as causative agent. It is posible that PQBP1 is firstly recruited by elongating RNAPII, then co-localizes to the assembling spliceosome through its C-terminal domain and, driven either by affinity or effective specificity, dynamic WW-mediated recognition may switch to SIPP1 binding to help activate the catalytic steps of pre-mRNA splicing. Alternatively, the role of RNAPII recognition may be secondary to the recognition of SIPP1, which has been shown to be shuttled to the nucleous independently from its own predicted nuclear localization signals, most possibly by PQBP1 (Llorian et al., 2005). Thus, under this model, PQBP1 functions as a scaffold between spliceosome assembly (C-terminal domain-mediated) and catalytic activity (WW-domain mediated).

This idea is apparently in paradox with the fact, that studies of PQBP1 involvement in intellectual disabilities using animal models show that *Mus musculus* and *Drosophila melanogaster* with knocked-down PQBP1 may be rescued from developing symptoms analogous to X-LID syndromes by applying HDAC inhibiting drugs (Ito et al., 2009; Tamura et al., 2010). Recent hypotheses of a cross-talk between chromatin remodelling and alternative splicing (Allemand et al., 2008) may shed

some light on these findings. In the later citation, the authors are "tempted to speculate that the splicing machinery relies on chromatin regulators which are able to read the 'histone code' to locate and access pre-mRNAs awaiting splicing". If they are given truth, the apparent paradox would turn to a further evidence.

Less conflictive are reports of PQBP1 transcription regulating activity through recognition of poly-Q expanded tracts in the transcription factors Brn-2 (Waragai et al., 1999) and ataxin-1 (Okazawa et al., 2002; Okuda et al., 2003). Indeed, SFs and TFs show common elements in their interaction networks and are oft erroneously categorized (Brès et al., 2005; Expert-Bezançon et al., 2002; Hastings et al., 2007). Poly-Q expanded ataxin-1 was shown to increases the affinity of the PQBP1-WW for the phosphorylated and active form of the RNAPII-CTD, leading to its dephosphorylation (Okazawa et al., 2002). Desphosphorylation on S2 and diffident reappearance of S5 phosphorylation on the CTD of eleongating RNAPII is known to slow down elongation rates and favor the recognition of weaker consensus sequences for splicing factor (de la Mata et al., 2003). Such situation favors the usage of alternative splicing patterns and the outcome of splicing variated gene products.

Thus, the empirical support for the involvement of PQBP1 in X-LID via alternative RNA splicing is found to fit and complement diverse empirical findings and theoretical postulates independently reported by different research laboratories.

REFERENCES

Allemand, E., Batsché, E., and Muchardt, C. (2008). Splicing, transcription, and chromatin: a ménage à trois. Curr. Opin. Genet. Dev. *18*, 145–151.

Bao, Y., Hata, Y., Ikeda, M., and Withanage, K. (2011). Mammalian Hippo pathway: from development to cancer and beyond. J. Biochem. (Tokyo) *149*, 361–379.

Batsché, E., Yaniv, M., and Muchardt, C. (2006). The human SWI/SNF subunit Brm is a regulator of alternative splicing. Nat. Struct. Mol. Biol. *13*, 22–29.

Beltrao, P., and Serrano, L. (2007). Specificity and Evolvability in Eukaryotic Protein Interaction Networks. PLoS Comput. Biol. *3*.

Bird, G., Zorio, D.A.R., and Bentley, D.L. (2004). RNA Polymerase II Carboxy-Terminal Domain Phosphorylation Is Required for Cotranscriptional Pre-mRNA Splicing and 3′-End Formation. Mol. Cell. Biol. *24*, 8963–8969.

Brès, V., Gomes, N., Pickle, L., and Jones, K.A. (2005). A human splicing factor, SKIP, associates with P-TEFb and enhances transcription elongation by HIV-1 Tat. Genes Dev. *19*, 1211–1226.

David, C.J., and Manley, J.L. (2011). The RNA polymerase II C-terminal domain. Transcription *2*, 221–225.

Dupont, S., Morsut, L., Aragona, M., Enzo, E., Giulitti, S., Cordenonsi, M., Zanconato, F., Le Digabel, J., Forcato, M., Bicciato, S., et al. (2011). Role of YAP/TAZ in mechanotransduction. Nature *474*, 179–183.

Expert-Bezançon, A., Caer, J.P.L., and Marie, J. (2002). HnRNP K is a component of an intronic splicing enhancer complex that activates the splicing of the alternative exon 6A from chicken- β-tropomyosin pre-mRNA. J. Biol. Chem.

Fairbrother, W., and Lipscombe, D. (2008). Repressing the neuron within. BioEssays *30*, 1–4.

Fu, J., Wang, Y.-K., Yang, M.T., Desai, R.A., Yu, X., Liu, Z., and Chen, C.S. (2010). Mechanical regulation of cell function with geometrically modulated elastomeric substrates. Nat. Methods *7*, 733–736.

Hastings, M.L., Allemand, E., Duelli, D.M., Myers, M.P., and Krainer, A.R. (2007). Control of Pre-mRNA Splicing by the General Splicing Factors PUF60 and U2AF65. PLoS ONE *2*, e538.

Hu, H., Columbus, J., Zhang, Y., Wu, D., Lian, L., Yang, S., Goodwin, J., Luczak, C., Carter, M., Chen, L., et al. (2004). A map of WW domain family interactions. PROTEOMICS *4*, 643–655.

Ito, H., Yoshimura, N., Kurosawa, M., Ishii, S., Nukina, N., and Okazawa, H. (2009). Knock-down of PQBP1 impairs anxiety-related cognition in mouse. Hum. Mol. Genet. *18*, 4239–4254.

Iwasaki, M., Tanaka, R., Hishiya, A., Homma, S., Reed, J.C., and Takayama, S. (2010). BAG3 directly associates with guanine nucleotide exchange factor of Rap1, PDZGEF2, and regulates cell adhesion. Biochem. Biophys. Res. Commun. *400*, 413–418.

Ladbury, J.E., and Arold, S. (2000). Searching for specificity in SH domains. Chem. Biol. *7*, R3–R8.

Lipscombe, D., Andrade, A., and Allen, S.E. (2013). Alternative splicing: Functional diversity among voltage-gated calcium channels and behavioral consequences. Biochim. Biophys. Acta BBA - Biomembr. *1828*, 1522–1529.

Llorian, M., Beullens, M., Lesage, B., Nicolaescu, E., Beke, L., Landuyt, W., Ortiz, J.-M., and Bollen, M. (2005). Nucleocytoplasmic Shuttling of the Splicing Factor SIPP1. J. Biol. Chem. *280*, 38862–38869.

Lubs, H., Abidi, F.E., Echeverri, R., Holloway, L., Meindl, A., Stevenson, R.E., and Schwartz, C.E. (2006). Golabi-Ito-Hall syndrome results from a missense mutation in the WW domain of the PQBP1 gene. J. Med. Genet. *43*, e30–e30.

Mahrenholz, C.C., Tapia, V., Stigler, R.D., and Volkmer, R. (2010). A study to assess the cross-reactivity of cellulose membrane-bound peptides with detection systems: an analysis at the amino acid level. J. Pept. Sci. *16*, 297–302.

De la Mata, M., Alonso, C.R., Kadener, S., Fededa, J.P., Blaustein, M., Pelisch, F., Cramer, P., Bentley, D., and Kornblihtt, A.R. (2003). A Slow RNA Polymerase II Affects Alternative Splicing In Vivo. Mol. Cell *12*, 525–532.

Mayer, B.J. (2001). SH3 domains: complexity in moderation. J. Cell Sci. *114*, 1253–1263.

Nasim, M.T., and Eperon, I.C. (2006). A double-reporter splicing assay for determining splicing efficiency in mammalian cells. Nat. Protoc. *1*, 1022–1028.

Neugebauer, K.M. (2002). On the importance of being co-transcriptional. J. Cell Sci. *115*, 3865–3871.

Okazawa, H., Rich, T., Chang, A., Lin, X., Waragai, M., Kajikawa, M., Enokido, Y., Komuro, A., Kato, S., Shibata, M., et al. (2002). Interaction between Mutant Ataxin-1 and PQBP-1 Affects Transcription and Cell Death. Neuron *34*, 701–713.

Okuda, T., Hattori, H., Takeuchi, S., Shimizu, J., Ueda, H., Palvimo, J.J., Kanazawa, I., Kawano, H., Nakagawa, M., and Okazawa, H. (2003). PQBP-1 transgenic mice show a late-onset motor neuron disease-like phenotype. Hum. Mol. Genet. *12*, 711–725.

Otte, L., Wiedemann, U., Schlegel, B., Pires, J.R., Beyermann, M., Schmieder, P., Krause, G., Volkmer-Engert, R., Schneider-Mergener, J., and Oschkinat, H. (2003). WW domain sequence activity relationships identified using ligand recognition propensities of 42 WW domains. Protein Sci. Publ. Protein Soc. *12*, 491–500.

Pawson, T., and Nash, P. (2000). Protein–protein interactions define specificity in signal transduction. Genes Dev. *14*, 1027–1047.

Phatnani, H.P., and Greenleaf, A.L. (2006). Phosphorylation and functions of the RNA polymerase II CTD. Genes Dev. *20*, 2922–2936.

Sudol, M. (2010). Newcomers to the WW Domain–Mediated Network of the Hippo Tumor Suppressor Pathway. Genes Cancer *1*, 1115–1118.

Sudol, M., and Harvey, K.F. (2010). Modularity in the Hippo signaling pathway. Trends Biochem. Sci. *35*, 627–633.

Sudol, M., Sliwa, K., and Russo, T. (2001). Functions of WW domains in the nucleus. FEBS Lett. *490*, 190–195.

Tamura, T., Horiuchi, D., Chen, Y.-C., Sone, M., Miyashita, T., Saitoe, M., Yoshimura, N., Chiang, A.-S., and Okazawa, H. (2010). Drosophila PQBP1 Regulates Learning Acquisition at Projection Neurons in Aversive Olfactory Conditioning. J. Neurosci. *30*, 14091–14101.

Tapia, V., Ay, B., Triebus, J., Wolter, E., Boisguerin, P., and Volkmer, R. (2008). Evaluating the coupling efficiency of phosphorylated amino acids for SPOT synthesis. J. Pept. Sci. Off. Publ. Eur. Pept. Soc. *14*, 1309–1314.

Tapia, V.E., Nicolaescu, E., McDonald, C.B., Musi, V., Oka, T., Inayoshi, Y., Satteson, A.C., Mazack, V., Humbert, J., Gaffney, C.J., et al. (2010). Y65C Missense Mutation in the WW Domain of the Golabi-Ito-Hall Syndrome Protein PQBP1 Affects Its Binding Activity and Deregulates Pre-mRNA Splicing. J. Biol. Chem. *285*, 19391–19401.

Ulbricht, A., Eppler, F.J., Tapia, V.E., van der Ven, P.F.M., Hampe, N., Hersch, N., Vakeel, P., Stadel, D., Haas, A., Saftig, P., et al. (2013). Cellular Mechanotransduction Relies on Tension-Induced and Chaperone-Assisted Autophagy. Curr. Biol. *23*, 430–435.

Volkmer, R., Tapia, V., and Landgraf, C. (2012). Synthetic peptide arrays for investigating protein interaction domains. FEBS Lett. *586*, 2780–2786.

Wada, K.-I., Itoga, K., Okano, T., Yonemura, S., and Sasaki, H. (2011). Hippo pathway regulation by cell morphology and stress fibers. Development *138*, 3907–3914.

Wang, Q., Moore, M.J., Adelmant, G., Marto, J.A., and Silver, P.A. (2013). PQBP1, a factor linked to intellectual disability, affects alternative splicing associated with neurite outgrowth. Genes Dev. *27*, 615–626.

Waragai, M., Lammers, C.-H., Takeuchi, S., Imafuku, I., Udagawa, Y., Kanazawa, I., Kawabata, M., Mouradian, M.M., and Okazawa, H. (1999). PQBP-1, a Novel Polyglutamine Tract-Binding Protein, Inhibits Transcription Activation By Brn-2 and Affects Cell Survival. Hum. Mol. Genet. *8*, 977–987.

Weiser, A.A., Or-Guil, M., Tapia, V., Leichsenring, A., Schuchhardt, J., Frömmel, C., and Volkmer-Engert, R. (2005). SPOT synthesis: reliability of array-based measurement of peptide binding affinity. Anal. Biochem. *342*, 300–311.

Appendix

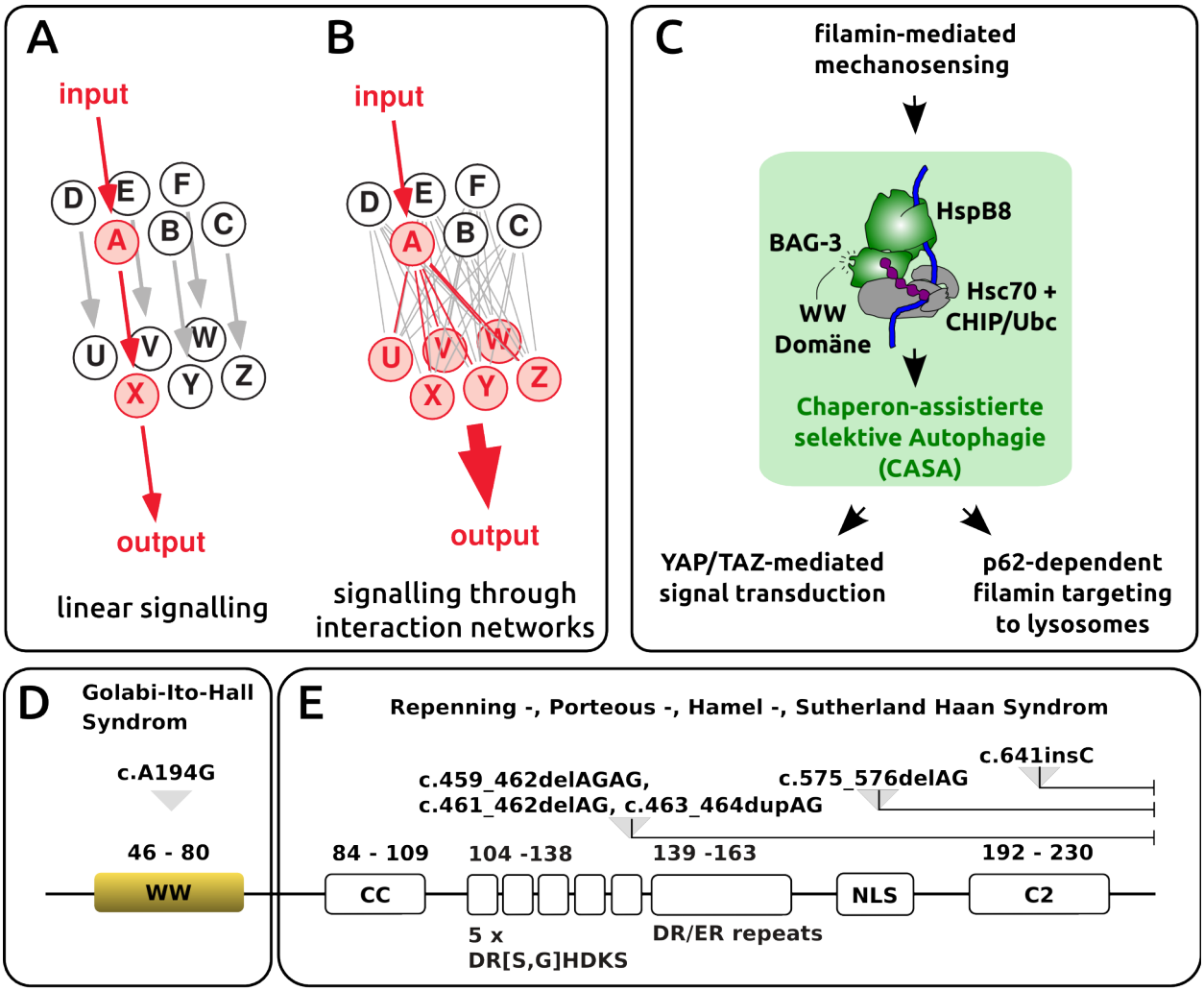

Figure 1 | Introductory illustrations. [A] Simplistic model of cellular signal transduction through a linear-chain of inherently specific binding events. Spots corresponding to the PPXY motifs carried by the SYNPO2, LATS1 and AMOTL2 proteins are marked with a red circle. [B] Specificity-free model of signalling through a network of various competing interactions orchestrated by factors globally affecting binding equillibria. From Mayer (2001). [C] State of the art in knowledge about CASA. [D] The single structured region of PQBP1 contains a WW domain. The c.A194G gene muattion translates in the Y65C single point mutation associated with the GIHS. [E] Six other gene mutations are shown, which cause truncation of the PQBP1 protein. All these truncated proteins lack the C2 domain, a domain known to bind splicing factors. Additionally, all these mutations, except for the c.641insC mutation in the Renpenning syndrome family, would give rise to a PQBP1 protein lacking or containing a disrupted nuclear localization signal (NLS) domain.

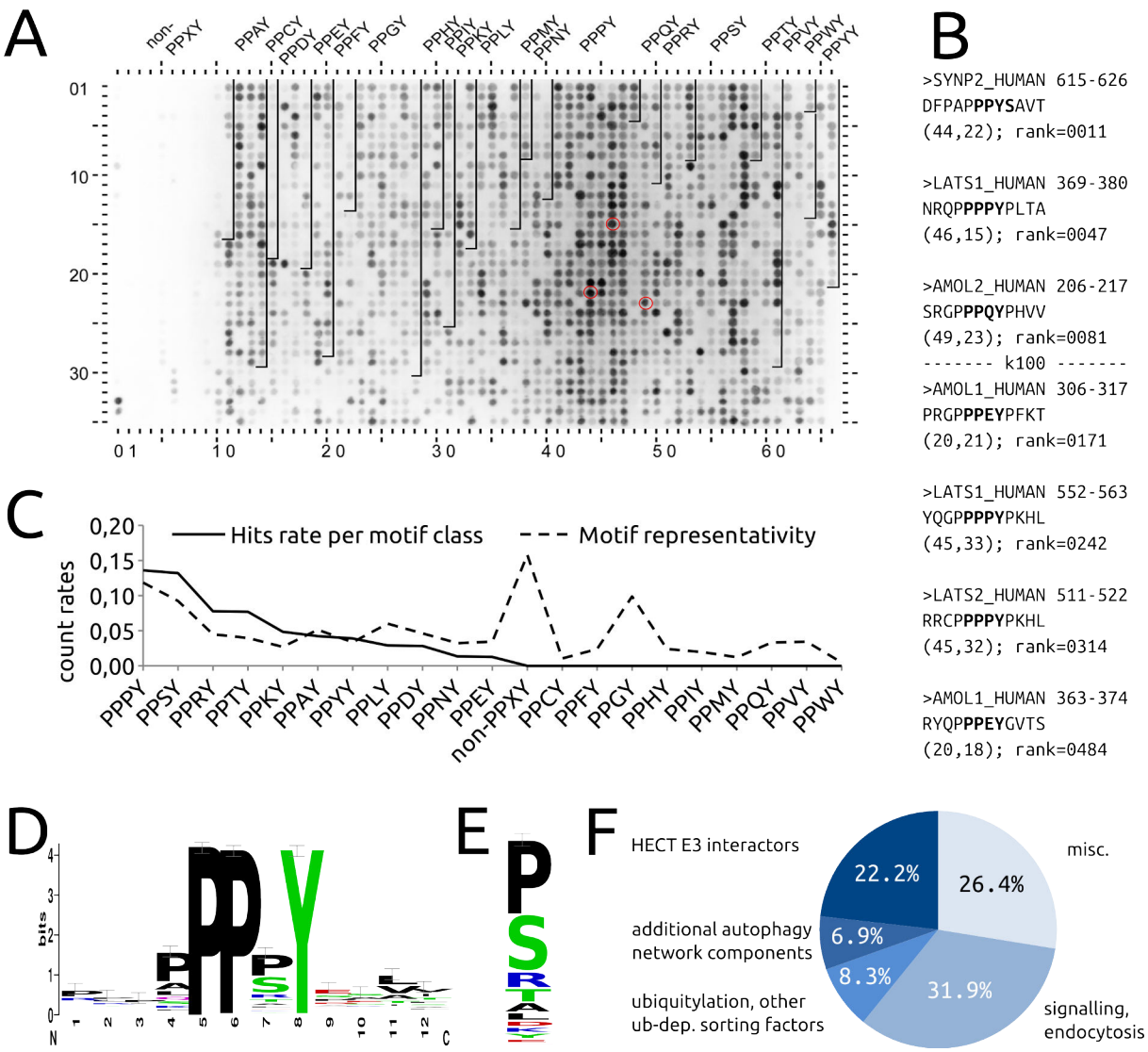

Figure 2 | BAG3 WW specificity profile. [A] Image record of probe reactivity. [B] Seven probes of interes. UniProt entry names, sequence positions, sequence, coordinates in panel A, and reactivity rank numbers are given. [C] Histogram of PPXY-class reactivities. Hits rate were calculated by counting reactive probes in each class and dividing by the number of probes in the class (blue bars). Representativity was calculated by dividing the number of probes in the class by the total number of probes in the assay (red bars). [D] Sequence Logo showing the scores of the position-weighted matrix for each amino acid in bits. [E] Position 7 in panel F is shown in more detail. [F] 72 of the 100 most reactive probes were succesfully blasted in UniProt. Gene ontologies and peer-reviewed literature was used to analyse the enrichment of biological processes.

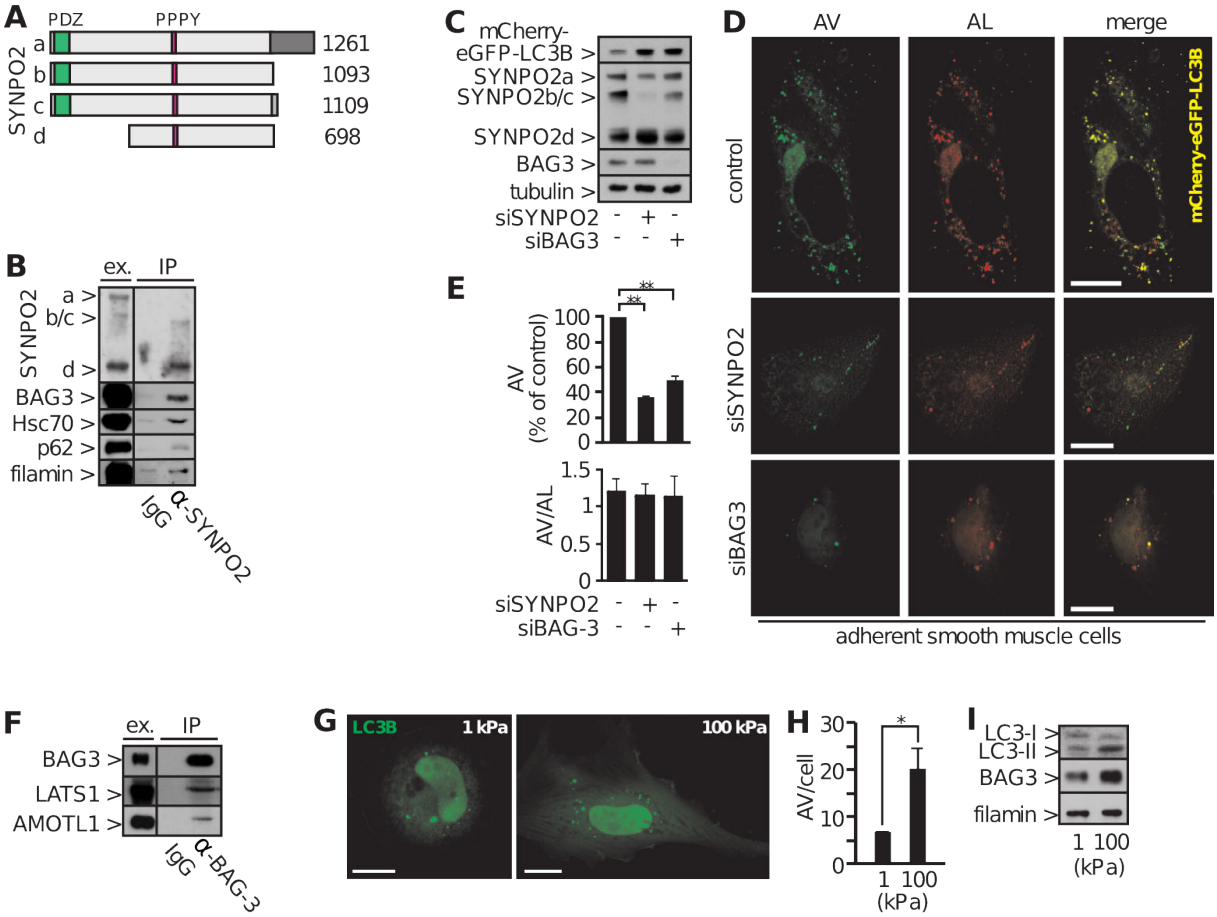

*Figure 3 | BAG3 in CASA. The BAG3 interactor SYNPO2 is recruited to CASA and is required for autophagosome formation (panels A-E). Concurrently, BAG3 coordinates CASA and YAP/TAZ regulation under mechanical tension (panels F-I). [A] Schematic presentation of SYNPO2 isoforms expressed in human cells. [B] Immuno-precipitation (IP) of SYNPO2 isoforms from A7r5 smooth muscle cells. Ex. - 60 µg of protein. [C] Smooth muscle cells were transfected with a plasmid encoding mCherry-eGFP-LC3B and with control, synpo2 or bag3 targeting siRNA for 72 h as indicated (-, siSYNPO2, siBAG3). (60 µg of protein per lane). [D] Autophagosome (AV, yellow signal in the merge) and autolysosome (AL, red signal in the merge) formation was monitored in adherent A7r5 cells expressing mCherry-eGFP-LC3B. When indicated SYNPO2 or BAG3 were depleted with corresponding siRNAS for 72 h prior to fixation. Scale bars: 20 µm. [E] Quantification of data obtained under panel A: Mean +/- SEM, n=3, and **P<0.01. [F] Immuno-precipitation (IP) of endogenous BAG3 from A7r5 rat smooth muscle cells reveals association with LATS1 and AMOTL1. Ex. - 60 µg of protein. [G] Fibronectin-coated elastomer substrates of different stiffness, i.e. 1 kPa versus 100 kPa, were used to induce different amounts of tension in adherent A7r5 smooth muscle cells. Autophagy was monitored after transfection with fluorescently labeled LC3B and grown under low and high tension for 16 h. Scale bars: 20 µm. [H] Quantification of data obtained under panel G: Mean +/- SEM, n=3, and *P<0.05. [I] Immuno-blot analysis of A7r5 cells grown under the same conditions as described under panel G.*

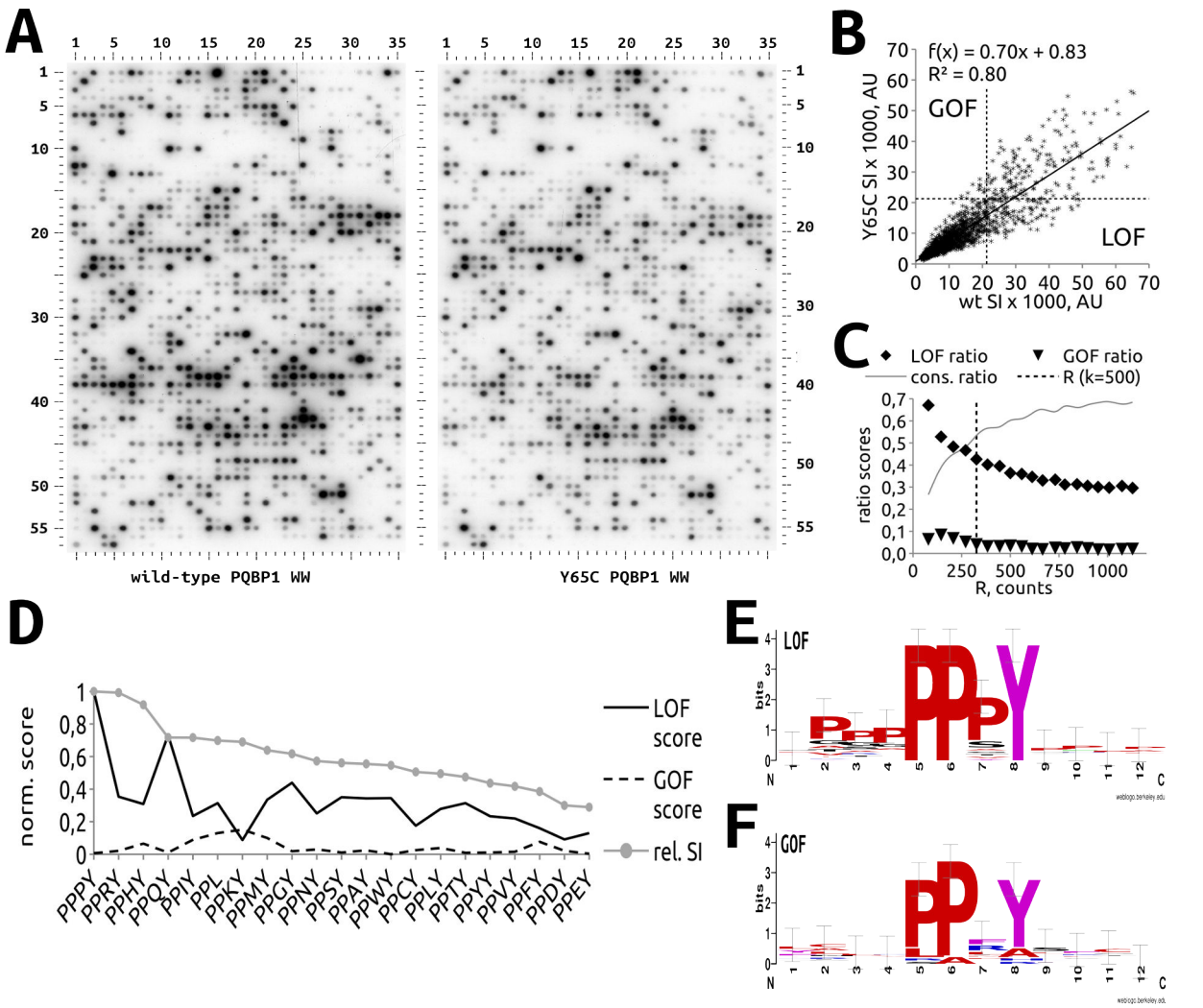

Figure 4 | Mutation effect on the PQBP1 specificity profile. [A] Direct comparison of the RIA films used to quantify analyte capturing of wild-type (left panel) and Y65C (right panel) PQBP1 WW to an equal set of probes. [B] Scatterplot of SI measurements with linear correlation analysis. The coefficient of determination was 0.80, showing the similarity of the Y65C specificity profile to the wild-type. Generally, an inclination of 0.70 of the regression line shows a weaker Y65C binding profile. Thresholds of SI used to define reactive probes and the mutation effect are also shown. SI thresholds are dependent on the number k of reactive events across both datasets. [C] The dependence of GOF and LOF scores on R is shown. The number R of reactive probes is defined as the set of probes with at least one reactive event across both datasets. Counts of R with unique binding event in the Y65C dataset are added to the gain-of-function score (GOF) and, similarly, R counts with unique wild-type reactivity are added to the loss-of-function score (LOF). [D] LOF and GOF scores of R(k=500) were counted for each PPXY motif class, normalized (a value of 1 means all counts in the class belong to the same score), and arranged on the plot according to descending relative signal intesity. [E] Sequence specificity of LOF probes by means of grafical logos. [F] Sequence specificity of GOF probes. Panels B, C, and D show that the mutation effect on probe recognition is most often observed as loss-of-function and rarely as gain-of-function. Panels E and F show that gain-of-function is based on recognition of non-cannonical motifs. The importance of proline in the context of the core motif is not observed in panel F. Additionally, positions 5, 6, and 8 in panel F depart from the maximal value of $log_2(20)$ idicating promiscuitive PPXY recognition. Less than 3% of total probes contained a non-cannonical PPXY motif, and yet they were often recognized by the Y65C WW domain.

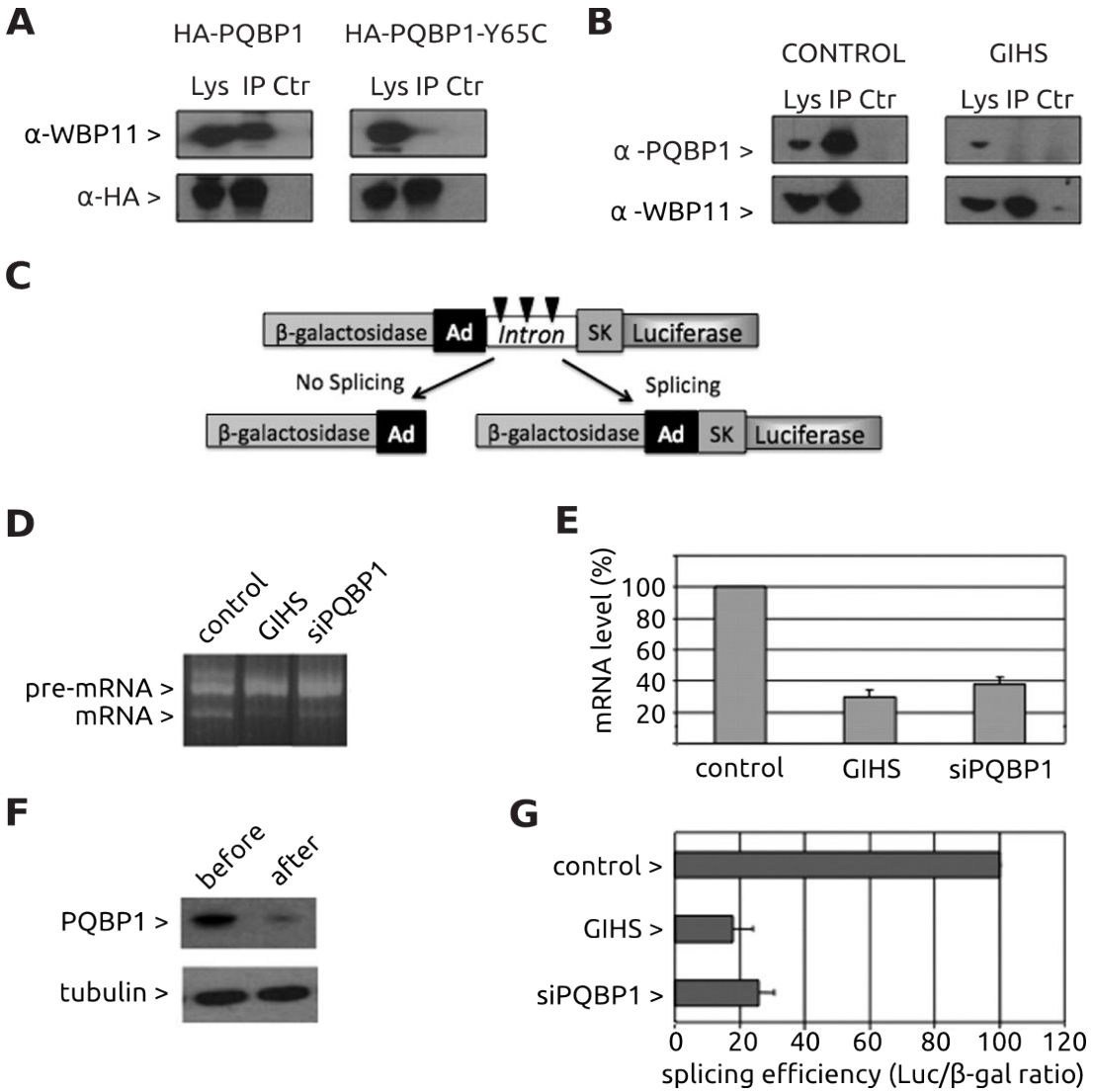

Figure 5 | Y65C PQBP1 in GIHS. PQBP1-Y65C shows a deficient interaction with WBP11 (panels A and B). In GIHS cells, splicing is impaired in a manner resembeling PQBP1-knocked-down cells (panels C-G). [A] EGFP-WBP11 was transiently expressed in HEK293T cells with either HA-PQBP1 or HA-PQBP1-Y65C. Subsequently, the lysate (Lys), anti-HA immunoprecipitates (IP) and control immunoprecipitates (Ctr) were used for immunoblotting with anti-WBP11 antibodies (anti-WBP11). [B] Immunoblots show that PQBP1 in but not PQBP1-Y65C co-immunoprecipitates with WBP11 from control- and GIHS patient-derived lymphoblast cell lysates, respectively. [C] Structure of the TN24 reporter construct. The β-galactosidase and luciferase reporter genes are fused in-frame but separated by an intronic sequence derived from the adenovirus (Ad) and the skeletal muscle isoform of human tropomyosin (SK). The intron contains three in-frame translation stop signals (indicated by three arrowheads). In the absence of splicing, β-galactosidase is generated. Splicing generates an active fusion of β-galactosidase and luciferase. [D] pre-mRNA and mRNA levels of the TN24 reporter plasmid in a representative experiment, as visualized after RT-PCR and electrophoresis on 2.5% agarose gels. [E] Relative transcript levels of the TN24 reporter plasmid, quantified by quantitative real-time-PCR. ACTIN was used as a normalization control for quantitative real-time-PCR. The data represent the means ± S.E. (n = 3). [F] Level of PQBP1 in cell lysates from healthy lymphoblasts before and after siRNA-mediated knockdown of PQBP1, as verified by immunoblotting. Tubulin was used as a loading control. [G] lymphoblasts from a healthy person before (control) or after knockdown of PQBP1 (siPQBP1) or from a GIHS patient (GIHS) were transiently transfected with the reporter plasmid TN24. The splicing efficiency of this reporter was assessed using the luciferase/β-galactosidase ratio. The data represent the means ± S.E. (n = 3) and are expressed as a percentage of the values obtained in control cells.

Eidesstattliche Versicherung

„Ich, VICTOR EDUARDO TAPIA MANCILLA, versichere an Eides statt durch meine eigenhändige Unterschrift, dass ich die vorgelegte Dissertation mit dem Thema: SPEZIFITÄTSPROFILE VON ERKENNUNGSDOMÄNEN IN DER MOLEKULAREN MEDIZIN selbstständig und ohne nicht offengelegte Hilfe Dritter verfasst und keine anderen als die angegebenen Quellen und Hilfsmittel genutzt habe.

Alle Stellen, die wörtlich oder dem Sinne nach auf Publikationen oder Vorträgen anderer Autoren beruhen, sind als solche in korrekter Zitierung (siehe „Uniform Requirements for Manuscripts (URM)“ des ICMJE -www.icmje.org) kenntlich gemacht. Die Abschnitte zu Methodik (insbesondere praktische Arbeiten, Laborbestimmungen, statistische Aufarbeitung) und Resultaten (insbesondere Abbildungen, Graphiken und Tabellen) entsprechen den URM (s.o) und werden von mir verantwortet.

Meine Anteile an den ausgewählten Publikationen entsprechen denen, die in der untenstehenden gemeinsamen Erklärung mit dem/der Betreuer/in, angegeben sind. Sämtliche Publikationen, die aus dieser Dissertation hervorgegangen sind und bei denen ich Autor bin, entsprechen den URM (s.o) und werden von mir verantwortet.

Die Bedeutung dieser eidesstattlichen Versicherung und die strafrechtlichen Folgen einer unwahren eidesstattlichen Versicherung (§156,161 des Strafgesetzbuches) sind mir bekannt und bewusst.“

_____

Datum Unterschrift

Anteilserklärung an den erfolgten Publikationen

Victor Tapia Mancilla hatte folgenden Anteil an den folgenden Publikationen:

Publikation 1: Mahrenholz, C.C., Tapia, V., Stigler, R.D., and Volkmer, R. **A study to assess the cross-reactivity of cellulose membrane-bound peptides with detection systems: an analysis at the amino acid level**. J. Pept. Sci. 16, 2010

Ich habe zur Entwicklung des Versuchsaufbaus, zur Durchführung der Versuche, zur Analyse der Daten und zur Überarbeitung des Textes beigetragen.

Publikation 2: Ulbricht, A., Eppler, F.J., Tapia, V.E., van der Ven, P.F.M., Hampe, N., Hersch, N., Vakeel, P., Stadel, D., Haas, A., Saftig, P., Behrends, C., Fürst, D.O., Volkmer, R., Hoffmann, B., Kolanus, W., and Höhfeld, J., **Cellular Mechanotransduction Relies on Tension-Induced and Chaperone-Assisted Autophagy,** Current Biology *23*, 2013

Ich habe zur Entwicklung des Versuchsaufbaus (Array-basierte Nachweisverfahren und präparativen Techniken), zur Durchführung der Versuche (Array-basierte Nachweisverfahren und präparative Techniken), zur Analyse der Daten (Spezifizitätsprofile) und zur Überarbeitung des Textes beigetragen.

Publikation 3: Tapia, V.E., Nicolaescu, E., McDonald, C.B., Musi, V., Oka, T., Inayoshi, Y., Satteson, A.C., Mazack, V., Humbert, J., Gaffney, C.J., Beullens, M., Schwartz, C.E., Landgraf, C., Volkmer, R., Pastore, A., Farooq, Bollen, M., and Sudol, M., **Y65C Missense Mutation in the WW Domain of the Golabi-Ito-Hall Syndrome Protein PQBP1 Affects Its Binding Activity and Deregulates pre-mRNA Splicing**, J. Biol. Chem. *285*, 19391–19401., 2010

Ich habe zur Entwicklung des Versuchsaufbaus (gesamte Strategie zusammen mit RV und MS), zur Versuchsdurchführung (Array-basierte Nachweisverfahren, präparative Techniken, SPR-basierte Bindungsassays, CD-Spektrometrie, "laser-light scattering" Spektrometrie, Entwicklung präparativer Methoden), zur Analyse der Daten (alle angegebene Methoden mit Ausnahme von "laser-light scattering"), und zur Überarbeitung des Textes beigetragen.

Unterschrift, Datum und Stempel des betreuenden Hochschullehrers/der betreuenden Hochschullehrerin

_____

Unterschrift des Doktoranden/der Doktorandin

_____

Publikation 1 – Mahrenholz et al., 2010

Mahrenholz, C.C., Tapia, V., Stigler, R.D., and Volkmer, R. (2010). A study to assess the cross-reactivity of cellulose membrane-bound peptides with detection systems: an analysis at the amino acid level. Journal of Peptide Science *16*, 297–302.

http://dx.doi.org/10.1002/psc.1237

Publication 2 – Ulbricht et al., 2013

Ulbricht, A., Eppler, F.J., Tapia, V.E., van der Ven, P.F.M., Hampe, N., Hersch, N., Vakeel, P., Stadel, D., Haas, A., Saftig, P., Behrends, C., Fürst, D.O., Volkmer, R., Hoffmann, B., Kolanus, W., and Höhfeld, J. (2013). Cellular Mechanotransduction Relies on Tension-Induced and Chaperone-Assisted Autophagy. Current Biology *23*, 430–435.

http://dx.doi.org/10.1016/j.cub.2013.01.064

Publication 3 – Tapia et al., 2010

Tapia, V.E., Nicolaescu, E., McDonald, C.B., Musi, V., Oka, T., Inayoshi, Y., Satteson, A.C., Mazack, V., Humbert, J., Gaffney, C.J., Beullens, M., Schwartz, C.E., Landgraf, C., Volkmer, R., Pastore, A., Farooq, A., Bollen, M., and Sudol, M. (2010). Y65C missense mutation in the WW domain of the Golabi-Ito-Hall syndrome protein PQBP1 affects its binding activity and deregulates pre-mRNA splicing. J. Biol. Chem. *285*, 19391–19401.

http://dx.doi.org/10.1074/jbc.M109.084525

Lebenslauf

Mein Lebenslauf wird aus datenschutzrechtlichen Gründen in der elektronischen Version meiner Arbeit nicht veröffentlicht

Publikationsliste

Spiess, M., E Verschueren, VE Tapia, PM Kim, A Norgaard, C Landgraf, R Volkmer, F Hochstenbach, B Distel, B Winsor, L Serrano, n.d. Evolution of SH3 domain mediated interaction networks. In progress.

Iglesias-Bexiga, M., Eva S. Cobos, Francisco Castillo, Tsutomu Oka, Virginia Mazack, Victor E. Tapia, Christiane Landgraf, Rudolf Volkmer, Marius Sudol, Irene Luque, n.d. Biophysical and Biochemical Analysis of the Binding of WW Domains of YAP Transcriptional Regulator to PPxY Motif-Containing Peptides of PATCHED and LATS Proteins. Submitted to Biophys. J.

Ulbricht, A., Eppler, F.J., Tapia, V.E., van der Ven, P.F.M., Hampe, N., Hersch, N., Vakeel, P., Stadel, D., Haas, A., Saftig, P., Behrends, C., Fürst, D.O., Volkmer, R., Hoffmann, B., Kolanus, W., and Höhfeld, J. (2013). Cellular Mechanotransduction Relies on Tension-Induced and Chaperone-Assisted Autophagy. Current Biology *23*, 430–435.

Volkmer, R., Kretzschmar, I., Tapia, V., 2012. Mapping receptor–ligand interactions with synthetic peptide arrays: Exploring the structure and function of membrane receptors. European Journal of Cell Biology 91, 349–356.

Volkmer, R., Tapia, V., Landgraf, C., 2012. Synthetic peptide arrays for investigating protein interaction domains. FEBS Letters 586, 2780–2786.

Volkmer, R., Tapia, V., 2011. Exploring Protein-Protein Interactions with Synthetic Peptide Arrays. Mini-Reviews in Organic Chemistry 8, 164–170.

Tapia, V.E., Nicolaescu, E., McDonald, C.B., Musi, V., Oka, T., Inayoshi, Y., Satteson, A.C., Mazack, V., Humbert, J., Gaffney, C.J., Beullens, M., Schwartz, C.E., Landgraf, C., Volkmer, R., Pastore, A., Farooq, A., Bollen, M., Sudol, M., 2010. Y65C missense mutation in the WW domain of the Golabi-Ito-Hall syndrome protein PQBP1 affects its binding activity and deregulates pre-mRNA splicing. J. Biol. Chem 285, 19391–19401.

Mahrenholz, C.C., Tapia, V., Stigler, R.D., Volkmer, R., 2010. A study to assess the cross-reactivity of cellulose membrane-bound peptides with detection systems: an analysis at the amino acid level. J. Pept. Sci 16, 297–302.

Tapia, V.E., Ay, B., Volkmer, R., 2009. Exploring and Profiling Protein Function with Peptide Arrays, in: Marina Cretich, Chiari, M. (Eds.), Peptide Microarrays. Humana Press, Totowa, NJ, pp. 3–17.

Tapia, V., Ay, B., Triebus, J., Wolter, E., Boisguerin, P., Volkmer, R., 2008. Evaluating the coupling efficiency of phosphorylated amino acids for SPOT synthesis. J. Pept. Sci 14, 1309–1314.

Tapia, V., Bongartz, J., Schutkowski, M., Bruni, N., Weiser, A., Ay, B., Volkmer, R., Or-Guil, M., 2007. Affinity profiling using the peptide microarray technology: A case study. Analytical Biochemistry 363, 108–118.

Weiser, A.A., Or-Guil, M., Tapia, V., Leichsenring, A., Schuchhardt, J., Frömmel, C., Volkmer-Engert, R., 2005. SPOT synthesis: Reliability of array-based measurement of peptide binding affinity. Analytical Biochemistry 342, 300–311.

Danksagung

Mit großer Vorfreude habe ich die Verleihung des Doktorgrades beantragt, denn die hier beschriebenen Leistungen erfüllen mich mit großen Stolz. Allerdings habe ich bei all der Freude und der spannenden Momente nicht aus den Augen verloren, dass ich nie soweit gekommen wäre, wenn mich nicht eine Vielzahl von Menschen auf meinem Weg begleitet und unterstützt hätte.

Daher möchte ich diese Gelegenheit nutzen, meinen tiefen Dank zum Ausdruck zu bringen.

Ich danke Dr. Rudolf Volkmer, der mir mit seinem Fachwissen zur Seite stand, viel Zeit für mich opferte und mir nicht zuletzt auch durch private Gespräche zu einem wertvollen und freundschaftlichen Wegbegleiter wurde.

Ich danke auch Dr. Klaus Gast, Prof. Sandro Keller, Dr. Marius Sudol sowie Prof. Jörg Höhefeld, die mir stets Ansprechpartner waren und meine Forschungsprojekte durch ihre Ideen, ihre Anregungen und ihre konstruktive Kritik bereicherten.

Ich danke besonders Fr. Ines Kretschmar und Fr. Christiane Landgraf, die mir viele Labortechniken sowie zahlreiche deutsche Sprüche lehrten und mich auch in angespannter und gestresster Laune ertrugen. In diesem Sinne: „Auch Wasser wird zum edlen Tropfen, mischt man es mit Malz und Hopfen“.

Und nicht zuletzt danke ich meine Lebenspartnerin, meinem Sohn und meinen Töchtern, die mir stets Mut zugesprochen haben. Ohne sie wäre meine Arbeit in dieser Form nicht möglich gewesen.